Biochimica et Biophysica Acta 1848 (2015) 1183–1195

Contents lists available at ScienceDirect

Biochimica et Biophysica Acta

journal homepage: www.elsevier.com/locate/bbamem

A refined atomic scale model of the *Saccharomyces cerevisiae* K^+-translocation protein Trk1p combined with experimental evidence confirms the role of selectivity filter glycines and other key residues

Vasilina Zayats [a,b], Thomas Stockner [c], Saurabh Kumar Pandey [a,b], Katharina Wörz [d], Rüdiger Ettrich [a,b,*], Jost Ludwig [a,d,*]

[a] Institute of Nanobiology and Structural Biology, Global Change Research Center, Academy of Sciences of the Czech Republic, Nove Hrady, Czech Republic
[b] Faculty of Sciences, University of South Bohemia, Nove Hrady, Czech Republic
[c] Institute of Pharmacology, Medical University of Vienna, Vienna, Austria
[d] Molecular Bioenergetics, Institute of Cellular and Molecular Botany, University of Bonn, Bonn, Germany

ARTICLE INFO

Article history:
Received 29 November 2014
Received in revised form 4 February 2015
Accepted 8 February 2015
Available online 14 February 2015

Keywords:
K^+-translocation
Eukaryotic Trk
Saccharomyces cerevisiae
Homology modeling
Molecular dynamics
Selectivity filter

ABSTRACT

Potassium ion (K^+) uptake in yeast is mediated mainly by the Trk1/2 proteins that enable cells to survive on external K^+ concentration as low as a few μM. Fungal Trks are related to prokaryotic TRK and Ktr and plant HKT K^+ transport systems. Overall sequence similarity is very low, thus requiring experimental verification of homology models. Here a refined structural model of the *Saccharomyces cerevisiae* Trk1 is presented that was obtained by combining homology modeling, molecular dynamics simulation and experimental verification through functional analysis of mutants. Structural models and experimental results showed that glycines within the selectivity filter, conserved among the K-channel/transporter family, are not only important for protein function, but are also required for correct folding/membrane targeting.

A conserved aspartic acid in the P_A helix (D79) and a lysine in the $M2_D$ helix (K1147) were proposed earlier to interact. Our results suggested individual roles of these residues in folding, structural integrity and function. While mutations of D79 completely abolished protein folding, mutations at position 1147 were tolerated to some extent. Intriguingly, a secondary interaction of D79 with R76 could enhance folding/stability of Trk1 and enable a fraction of Trk1[K1147A] to fold.

The part of the ion permeation path containing the selectivity filter is shaped similar to that of ion channels. However below the selectivity filter it is obstructed or regulated by a proline containing loop. The presented model could provide the structural basis for addressing the long standing question if Trk1 is a passive or active ion-translocation system.

1. Introduction

Potassium (K^+) ions are the most abundant ion species in almost all living cells. In non-excitable cells, K^+ e.g. provides favorable conditions for many enzymatic reactions and serves as osmoticum. In excitable cells K^+ ions play an important role in signal transduction and modulation of signaling processes. Voltage-gated K-channels of the *Shaker* type e.g. are the most diverse class of ion transport systems known (see e.g. [1]).

Baker's yeast (*Saccharomyces cerevisiae*) cells are able to grow in environments with a wide range of external [K^+] ranging from less than 100 μM to more than 1 molar. The internal [K^+] is maintained relatively constant by a variety of cation transport systems in the plasma - and organellar membranes of *S. cerevisiae* (for review see e.g. [2]). At high (>20 mM) $[K^+]_{ext}$, cells are able to take up the necessary amount of K ions by a so called "ectopic uptake system" [3,4] that probably consists of unspecific transport through amino acid and sugar permeases. In addition, a molecularly not yet identified "non specific cation channel", Nsc1 [5] might play a role. Surplus K^+ is exported via the $(Na^+/K^+)/H^+$ antiporter Nha1 and the ATPase Ena1(−5) or sequestered in the vacuole. At low $[K^+]_{ext}$ Trk1 [6] is the most important specific K^+ uptake system. Cells lacking that gene are (depending on pH) not able to grow on external [K^+] < ~3–20 mM [6,7].

The structure of Trk1 was initially assumed to be similar to those of the "major facilitator superfamily" (MFS) i.e. consisting of 12 TM domains and a large hydrophilic loop located either intra- or extracellular. It was also assumed that in analogy to many members of the MFS family, transport was secondary active and driven by co-transport with H^+. However, sequence analysis revealed an evolutionary

* Corresponding authors at: Institute of Nanobiology and Structural Biology, Global Change Research Center, Academy of Sciences of the Czech Republic, Nove Hrady, Czech Republic. Tel.: +420 389 033 844; fax: +420 386 361 279.
E-mail addresses: ettrich@nh.cas.cz (R. Ettrich), jost.ludwig@uni-bonn.de (J. Ludwig).

http://dx.doi.org/10.1016/j.bbamem.2015.02.007
0005-2736/

relationship between KcsA and Ktr/Trk/HKT-type transport systems [8] and K-channels (KcsA, [9]). According to this prediction Trk proteins evolved via gene duplication from a single monomer of a KcsA like channel. Therefore Trk consists of one single polypeptide chain with four joint units homologous to KscA, each of them containing of two transmembrane helices, M1 and M2, connected via pore helix and selectivity filter loop. All Ktr/Trk/HKT-type proteins were assumed to preserve a similar K^+ selective filter with conserved Gly residues and transmembrane protein architecture. Corresponding models of each member of the K^+ transport systems family were developed based on the (crystal) structure of KcsA [10].

However, these models provide only medium resolution structures as they are based on a template with sequence identity below 15%. Additionally the resulting structures lack systematic experimental verification. Several studies involving site directed mutagenesis were since then performed to elucidate the ion translocation pathway, the transport mechanism and also the role of the unusually high number of charged residues in Trk1 $M2_D$ helix [11–13]. But the results were not entirely conclusive.

Recently, the crystal structures of Ktr/Trk/HKT-type transporters, TrkH [14] and KtrB [15], were solved. These structures supported earlier predictions about the similarity of their respective selectivity filters with that of K^+ channels and the conservation of the glycine residues [10]. The overall structures also revealed major differences between TrkH/Ktrb and KcsA and provided a better ground for structural homology modeling of *S. cerevisiae* Trk1 as an example for a eukaryotic Trk K^+ translocation system. Although Trk1 is regarded closer related to TrkH than KcsA [8], it shows a sequence identity of only 11%. However, KtrB shows a sequence identity of ~22% to Trk1, supporting the prediction of a conserved fold thereby justifying the use of the structure based homology modeling approach. Both structures were available for model building, which allowed for a better identification of structurally and sequentially conserved and variable regions. The structural information were augmented with bioinformatic analyses. Initial atomic level models of Trk1 were prepared on the basis of the TrkH and KtrB structures. The models were subsequently tested by molecular dynamics simulations in a membrane environment and scrutinized further by experimentally evaluating predictions.

2. Methods

2.1. Yeast strains, media and growth tests

Haploid *S. cerevisiae* yeast strains used throughout this study are listed in Table 1. Strains were grown aerobically at 28 °C with rotational shaking at 250 rpm in liquid synthetic medium (Synthetic dextrose arginine phosphate, SDAP, [16]) with 2% D-glucose, supplemented with the appropriate amino acids. The medium was adjusted to pH 5.9 with phosphoric acid (SDAP) and supplemented with the appropriate amount of KCl. All media were prepared with ultrapure (MilliQ) water.

Table 1
S. cerevisiae strains used in this study. Within the text mutations ([mut]) are denominated in the form original [OnnnnN] (, OnnnnN, …) with O and N indicating the original and new residue in one letter code and nnnn being the position in the *S. cerevisiae* Trk1 amino acid sequence. An overview of all mutations is given in supplementary Fig. 3.

Name	Genotype	Reference
BY4741	*MATa his3Δ1 leu2Δ0 met15Δ0 ura3Δ0*	[48]
BY4741-3M (BY4741 Δ*trk1,2,tok1*)	*BY4741 trk1::loxP, trk2::loxP, tok1::loxp*	[49]
BY4741 Δtrk1,2	*BY4741 trk1::loxP, trk2::loxP*	[50]
BY4741-3M-TRK1	*BY4741 Δtrk1,2, tok1::* LEU2, P_{CDR1}-TRK1 (*p77T-P_{CDR1}-TRK1*)	This study
BY4741-3M-fnc (functional negative control)	*BY4741 Δtrk1,2, tok1::* LEU2, P_{CDR1} (*p77T-P_{CDR1}*)	This study
BY4741-3M-TRK1/GFP	BY4741-3M [pYEX-TRK1/GFP]	This study
BY4741-3M-TRK1[mut]	*BY4741 Δtrk1,2, tok1::* LEU2, P_{CDR1}-TRK1[mut] (*p77T-P_{CDR1}-TRK1[mut]*)	This study
BY4741-3M-TRK1[mut]/GFP	BY4741-3M [pYEX-TRK1[mut]/GFP]	This study

2.1.1. Growth tests

The growth capacity in solid media was studied on SDAP plates supplemented with different KCl concentrations. 1.5 μL of dilution series ranging from an OD of 1 to 0.01 of cultures were spotted on the plates. Pictures were taken after 3 to 5 days incubation at 28 °C. In some of the figures shown below, dilution dot series were re-arranged to allow for easier comparison between mutants.

2.2. Potassium uptake measurements

K^+ uptake was analyzed using a potassium selective electrode (C-CCIT, Wädenswil, Switzerland) and a 2 M $MgSO_4$ filled reference electrode (C-CIT). Voltage was measured using a pH-meter (PHM92, Radiometer, Copenhagen, Denmark) as high impedance amplifier. Data was recorded at 2 Hz using an A/D converter (U12, LabJack, Lakewood, Colorado, USA) and RealView 3.0 software (Abacom, Ganderkesse, Germany). Raw data was median filtered (2.5 sec) and subsequently smoothed by a spline fit using R 2.15 (http://www.r-project.org). Calibrations were carried out using KCl standards using at least six concentrations from 0.001 to 10 mM KCl.

For measurements cells were grown to stationary phase in SDAP medium, harvested by centrifugation (4000 ×*g*, 5 min) and washed twice in the two-fold volume of the original culture in water. Subsequently cells were re-suspended in water (2-fold volume of the original culture volume), "starved" by continuous stirring at 4 °C over night, harvested, washed once more (water, 2-fold original culture volume) and resuspended to a density of 1.2×10^9 cells/mL in water. Measurements were carried out at room temperature in a total volume of 2 mL in 50 mM Tris/Citrate pH 5.0, 0.2 mM KCl, and 1.2% (w/v) glucose and additional ions when desired. Experiments were started by addition of cells to a density of 1.14×10^8 cells/mL. Data was evaluated from cell addition for 20 min.

2.3. Molecular biology

2.3.1. Plasmids and constructs

p77T-P_{CDR1} was derived from p679 [17] using standard molecular biology techniques by (i) replacing the 5′ and 3′ sequences directing integration into the LEU2 locus with corresponding sequences from TOK1, (ii) replacing HIS3 cassette with a LEU cassette and (iii) introducing the CDR1 promoter from *Candida albicans* resulting in p77T-P_{CDR1}. p77T-P_{CDR1}-TRK1 was generated by cloning the TRK1 coding sequence into p77T-P_{CDR1}. A schematic map of p77T-P_{CDR1}-TRK1 is shown in Supplementary Fig. 1. The full sequence is available from the authors.

pYEX-TRK1/GFP is a pYEX-BX (Clontech Laboratories, Mountain View, CA, USA) based plasmid in which a TRK1/GFP fusion genes expression is driven by the metallothionine promoter P_{CUP}. A schematic map of pYEX-TRK1/GFP is shown in Supplementary Fig. 2. The full sequence is available from the authors.

2.3.2. In vitro mutagenesis

Mutagenesis was performed using the overlap extension method [18]. Mutagenised fragments were back-cloned into the original plasmids using suitable restriction enzymes. All PCR derived parts of the constructs were fully sequenced to ensure the presence of the desired and the absence of unwanted mutations.

2.3.3. Transformation and verification of yeast strains

Yeast cells were transformed according to [19]. Integrative (p77T) constructs were digested with *Not*I before transformation, yielding linear

DNA fragments with 5′- and 3′ integration directing sequences exposed at the respective ends. Correct integration was checked by analytical PCR using 2 sets of primer pairs: (i) a construct internal antisense primer vs. a 5′ primer upstream of the integration site and (ii) a construct internal sense primer within the integration construct and an external antisense primer.

Strains derived by transformation with pYEX-TRK1([mut])/GFP constructs were verified and analyzed by fluorescence microscopy.

2.4. Fluorescence microscopy

Fluorescence microscopy was carried out using a Nikon Eclipse 80i fluorescence microscope with Nikon Plan Fluor 100×/1.30 oil immersion lens (Kurobane Nikon, Tochigi, Japan) and a filter set consisting of 450–490 nm excitation, 505 nm beam splitter and 520 nm longpass for emission. Pictures were taken using a cooled CCD camera (Vosskühler CCD 1300, VDS-Vosskühler, Osnabrück, Germany) and Nikon NIS-Elements software.

2.5. Sequence analysis and homology modeling

A multiple sequence alignment between members of Trk/Hkt/Ktr families was built initially using several alignment tools, including ClustalW [20], T-Coffee [21], Expresso [22]. These alignments were merged and manually adjusted by taking secondary structure predictions and structural information of available templates into account. Models of several members of the Trk family were developed. The correct alignment must allow for model building of all members of the Trk family. Candidate alignments that resulted in models incompatible with protein stability criteria could thereby be detected and excluded. The final alignment (Fig. 1) thus represents a consensus of all available information.

Several models using different templates were generated using Modeller [23]. An initial model of Trk1 was built based on TrkH structure (PDB ID: 3PJZ) despite the low sequence identity (11 %), as this was the first available template of Trk/Hkt family. Later the crystal structure of the structurally more closely related KtrB template (PDB ID: 4J7C) with a sequence identity of 22 % became available and was used to refine the Trk1 model.

The quality of model geometry was assessed using Ramchandran plots and G-factor calculations in PROCHECK [24]. Additionally, the theoretical correctness of the structure was validated using the Modeller objective function, the discrete optimized protein energy score (DOPE) [25] and the protein structure analysis tool ProSa, which estimates the structural model quality [26]. The best structure out of 100 models was selected for further analyses. In order to assess the quality of the dimeric structure, hydrophobic contacts were identified between the two monomers in the final Trk1 dimer. Hydrophobic interactions were defined between pairs of nonpolar carbon or sulfur atoms that are separated by <5 Å and are not 1–4 bonded. 161 of such interactions were found. PDB coordinates of the model are available upon request from the authors.

2.6. Molecular dynamics

The selected model was embedded into a pre-equilibrated POPC (1-palmitoyl-2-oleoyl-sn-glycero-3-phosphocholine) bilayer consisting of 512 lipid molecules using the inflategro method [27]. Berger lipids [28], converted into the format of the OPLS (Optimized Potentials for Liquid Simulations) all-atom force field [29] following the procedure proposed by Neale & Pomès (2006) [30], were used to describe the POPC molecules. The OPLS all-atom force field was used in all simulations to describe the protein. Water was represented by the simple point charge (SPC) [31] water model. All simulations were performed using the Gromacs 4.6 molecular dynamics package [32–34]. The integration time step was set to 2 fs. Periodic boundary conditions were applied in all dimensions. The neighbor search list was updated every 10 steps. A constant temperature of 300 K was maintained using the Berendsen thermostat [35] and a coupling time of 0.1 ps, coupling independently water, membrane and the protein to an external bath. A pressure of 1 bar was maintained semi-isotropically, using the Berendsen pressure coupling scheme [35] with a time constant of 4 ps. Bond lengths were constrained using the linear constraint solver algorithm (LINCS) method [36]. A cutoff of 1.0 nm was applied for Van der Waals (VdW) interactions. Long-range electrostatic interactions were calculated according to the particle mesh Ewald (PME) method [37], using a cutoff of 1 nm. The reciprocal space interactions were evaluated on a 0.14 nm grid using B-splines of fourth order.

3. Results

3.1. Experimental system

In order to establish an easy to handle system to test the function of Trk1, we integrated TRK1 under control of the (in *S. cerevisiae* constitutively active) *Candida albicans* CDR1 promoter (P_{CDR1}) into the TOK1 locus of a strain lacking *trk1* and *trk2*, resulting in strain BY4741-3M-TRK1 possessing only Trk1 as K^+-uptake system. This strain was also leucine auxotroph. It has been shown that auxotrophies strongly affect the physiology of yeast growth [38]. Therefore we generated the strain BY4741-3M-fnc as a negative control that does not express TRK1 but is otherwise isogenic to BY4741-3M-TRK1. Growth tests on solid media were performed (not shown) with [KCl] from 0.01 mM to 100 mM as functional test for Trk1 activity. They revealed that the K^+ requirements of BY4741-3M-TRK1 and BY4741-3M-fnc were very similar to those of BY4741 and the strain lacking *trk1*, *trk2* and *tok1* (BY4741-3M). As expected, BY4741-3M-TRK1 exhibited good growth on media with low [KCl] (0.1–1 mM), whereas BY4741-3M-fnc only grew significantly, when [K^+] was higher than 1 mM (Figs. 7, 9, 11).

To analyze the membrane targeting, initially a strain in which the TRK1/GFP fusion protein was expressed under control of P_{CDR1} was prepared. However, we were not able to detect fluorescence. Therefore subsequently strain BY4741-3M-TRK1/GFP was constructed by transforming BY4741-3M with the multicopy plasmid pYEX-TRK1/GFP. Fluorescence microscopy showed that the major portion of the Trk1/GFP fusion protein was localized at the cell periphery, likely at the plasma membrane (Fig. 2). Thus strain BY4741-3M-TRK1[mut]/GFP was suitable to monitor targeting of Trk1 mutants.

3.2. Modeling and testing of models

The overall Trk1 structure in our model (Fig. 3) resembles closely the general fold of potassium channel pores with the difference that instead of four identical protomers, the Trk1 has four domains (A-D) on one peptide chain. Each Trk1 domain corresponds to one potassium channel monomer (Fig. 3).

The four domains assemble around a central axis and form the pore (Fig. 4). Each repeat includes a M1 helix followed by the P-loop region including the pore helix and the selectivity filter sequence. A significant deviation from potassium channel structures is seen within the M2 helix that we modeled following the KtrB template. It consists of two helices: the first one is short, ending close to the center of the membrane, followed by a short bend of nearly 90 degrees that includes a proline residue in each of the repeats. The second helix is aligned almost parallel to the membrane moving away from the central transporter axis. Four glycine residues (G92, G831, G959 and G1126) are located at the narrow end of the funnel shaped selectivity filter, with a distance of approximately 5.8 and 5.6 Å between opposite C-α atoms (Fig. 3). The electrostatic potential (ESP) is negative in the extracellular part of the protein, thereby supporting increased cation density above the selectivity filter (Fig. 4). The largest negative values, as indicated by the most intense red color are located in the center of each monomer right above the selectivity filter (Fig. 4).

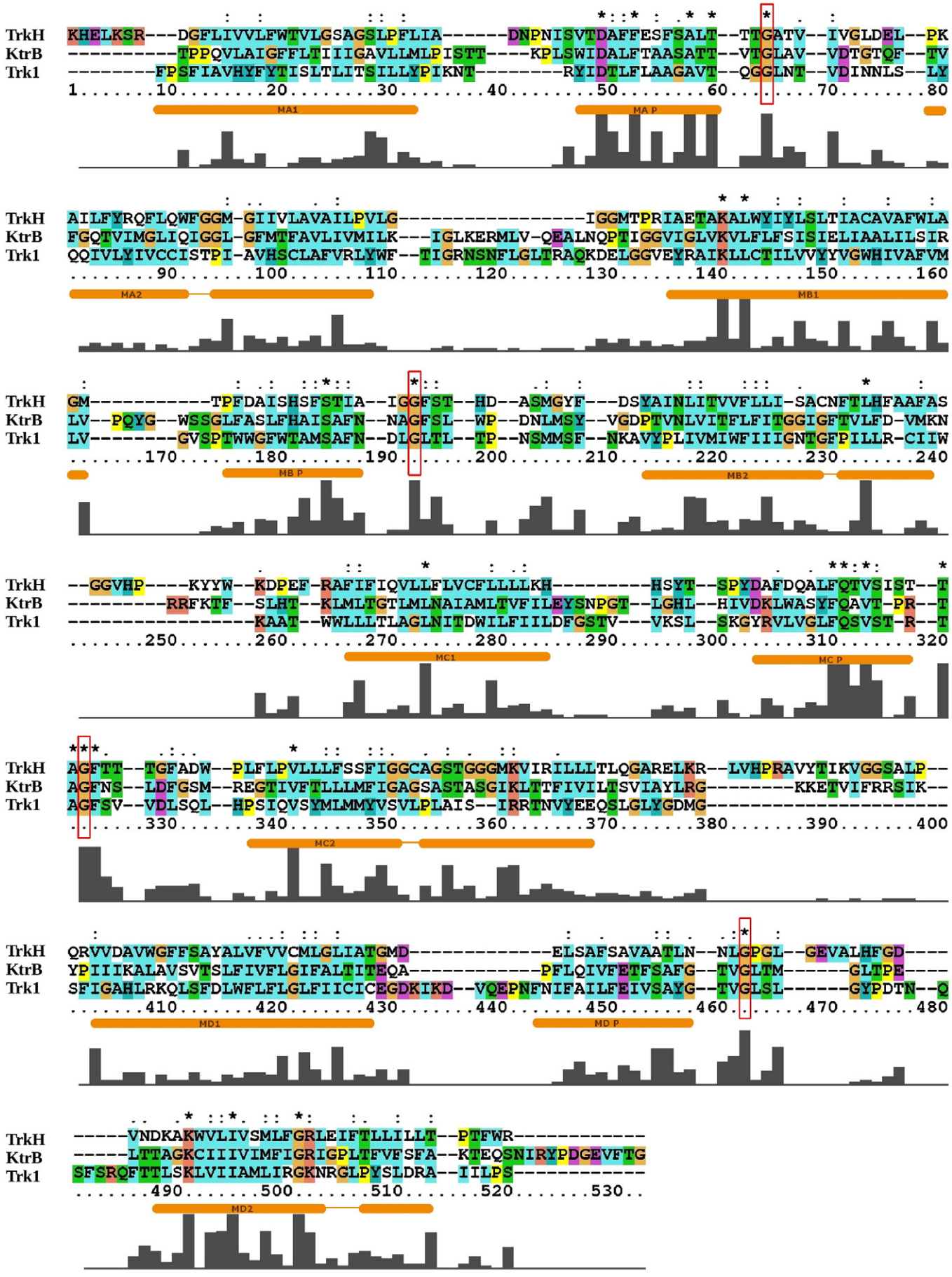
TrkH
KtrB
Trk1
MA1
MA P
MA2
MB1
MB P
MB2
MC1
MC P
MC2
MD1
MD P
MD2

As in the closest structural homolog KtrB, the bend in M2 in the third (C) domain is longer than in the other three domains and has been modeled as an intramembrane loop in Trk1 to match the KtrB architecture (Fig. 3). This nine residue long loop is very hydrophobic as it contains two leucine, two isoleucine, one valine, one alanine, two serine and one proline residue. This loop fills the space between the selectivity filter and the cytoplasmic pore, thereby blocking the ion permeation path. A cut through the protein molecular surface (Fig. 5) shows the central volume of the protein occupied by this internal loop. A transition to the open conformation of Trk1 will require a rearrangement in this region to allow transport. The electrostatic surface potential (Fig. 5) is most negative at the pore entrance and the selectivity filter, whereas becoming positive towards the intracellular site.

The state of our model corresponds to the closed conformation of the KtrB and TrkH crystal structures. Trk1 was modeled as a dimer, following the templates, with a hydrophobic dimer interface of 1300 Å^2. The sequence identity with the template in the modeled transmembrane region is 22% as calculated over the averaged length of the two sequences using the SIAS server [39]. The final model shows 91.4 % of all residues in highly favored and favored regions and 0.8 % of residues in disallowed regions. The ProSa result (Supplementary Fig. 4) demonstrates a favorable z-score (−2.45) throughout the whole protein.

In 100 ns MD simulations the modeled transmembrane segments and the secondary structure were stable as can be seen from the secondary structure analysis over time (Supplementary Fig. 5). RMSD values calculated for C-α of the transmembrane segments of the individual domains reached a plateau in the range from 1.5 Å to 1.9 Å indicating that no major conformational changes in tertiary structure occurred during the simulations.

3.3. Mutations in putative key residues

3.3.1. Putative selectivity filter glycines

As mentioned already, potassium transporters and potassium channels share the same ancestor. The glycine residues in the selectivity filter are key residues that allowed sequence matching the sequences of the prokaryotic K-channel KcsA and K^+ transporters (Fig. 1, 3). These residues were also the basis for matching pore helices and transmembrane helices in the earlier models. The correct alignment of the conserved selectivity filter glycine residues was confirmed by the crystal structures of TrkH and KtrB [14,15]. Mutagenesis studies with HKT and KtrB [40–42] showed that mutations of these glycines alter ion selectivity. However, the positions of the selectivity filter glycines have not yet been experimentally verified for *S. cerevisiae* Trk1. Therefore, we mutated the four putative glycines (G92, G831, G959, G1126) in the selectivity filter. These four glycine residues were changed to bulky residues (leucines) one by one because we intended to rule out, that these glycines were incorrectly aligned and could be located outside the selectivity filter. Growth tests showed that none of the generated strains was able to grow on low [KCl] containing plates (not shown). Furthermore, fluorescence microscopy with the corresponding TRK1/GFP fusion gene expressing strains showed that the mutated fusion proteins were not correctly folded or targeted to the plasma membrane. This suggested that residues with spacious side chains (like leucine) at this position might result in a steric clash within the structure, prohibiting proper protein folding (Fig. 6).

Next, more conservative mutations were introduced at the positions of the presumed selectivity filter glycines by replacing them one by one with alanine having a small side chain. It was expected that the overall structure of Trk1 would be able to tolerate this relatively small change. Replacement of the selectivity filter glycines in domains A, B and C exerted only a relatively minor effect on targeting/folding of the Trk1/GFP fusion proteins. The substitution of the glycine in domain D (G1126A) partially impaired protein folding/targeting (Fig. 7) though to a much lower degree than the leucine substitutions.

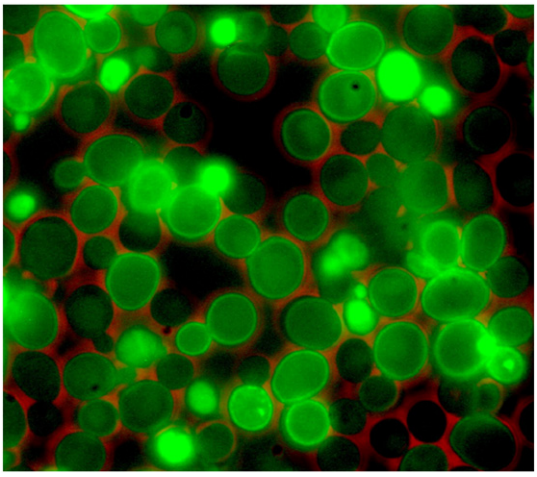

Fig. 2. *Trk1/GFP fusion protein expressed from pYEX-TRK1/GFP is localized at the cell periphery, most likely the plasma membrane*. Shown is the overlay of GFP fluorescence (green channel) and the corresponding bright filed image (red channel).

Functional tests (Fig. 7) showed that all glycine to alanine mutants had growth defects at low external [K^+]. However, Trk1[G959A] and [G92A], grew clearly better than [G831A] and [G1126A]. Surprisingly all four mutated proteins also led to severely inhibited growth at "permissive" high [K^+], i.e., in which there was no growth difference observed between the negative control strain BY4741-3M-fnc and the "wt" strain BY4741-3M-TRK1. To more directly assess the function of the mutated Trk1 proteins in comparison to wt, we performed K^+-uptake experiments by analyzing the decrease of K^+ in the external buffer ($[K^+]_{ext}$) using K^+ selective electrodes (Fig. 8). The selectivity filter glycine to alanine mutation, G959A (SF_C) was selected as an example, because growth at low [K^+] was observed and also targeting/folding was almost indistinguishable from wt. In general $[K^+]_{ext}$ decrease was lower with G959A than with wt what might be explained by a still slightly lower amount of functional G959A compared to wt. When Na^+ in addition to 0.2 mM K^+ was present, both $[K^+]_{ext}$ decrease mediated through wt and G959A were diminished in a concentration dependent manner. However, the effect was much stronger in G959A. Whereas wt expressing cells were able to take up K^+ even in the presence of 20 mM NaCl, G959A cells lost K^+ under the same conditions. In addition, the presence of 2 mM $CaCl_2$ affected G959A expressing cells much more than wt expressing cells. 30 mM ChCl significantly inhibited G959A, but did not decrease K^+ uptake of wt expressing cells. Similar results were observed with Trk1[G92A] (not shown). This result could indicate changes in pore or selectivity filter structures. Thus, in order to study the structural effect of a glycine to alanine mutation, we conducted 100 ns molecular dynamics simulations with G959A. The mutation did not affect the overall protein structure stability as determined by secondary structure analysis and root mean square deviation. However, we observed an increase in size of the selectivity filter, from 5.8 Å (wt) to 7.5 Å (G959A) measured between opposite glycine (alanine) Cα atoms across the ion permeation pore (domains A-C, B-D).

3.3.2. Observed electrostatic interactions

Within the $M2_D$ helix and the P_A loop, a lysine (K1147 in Trk1) and an aspartate (D79 in Trk1) are strongly conserved throughout Trk1,2/KtrB/TrkH/HKT families (Fig. 1). The crystal structures of TrkH and

Fig. 1. *Alignment of the core, i.e. transmembrane regions of S.c. Trk1 with KtrB (4j7c) and TrkH (3pjz)*. Identical residues are indicated by an asterisk; colon (:) and periods (.) indicate conserved positions with similar properties, respectively. Positions of selectivity filter glycines are indicated by red boxes. Transmembrane helices of all subunits are underlined by thick orange colored lines. Sequences are colored according to automatic calculated alignment consensus (ClustalX).

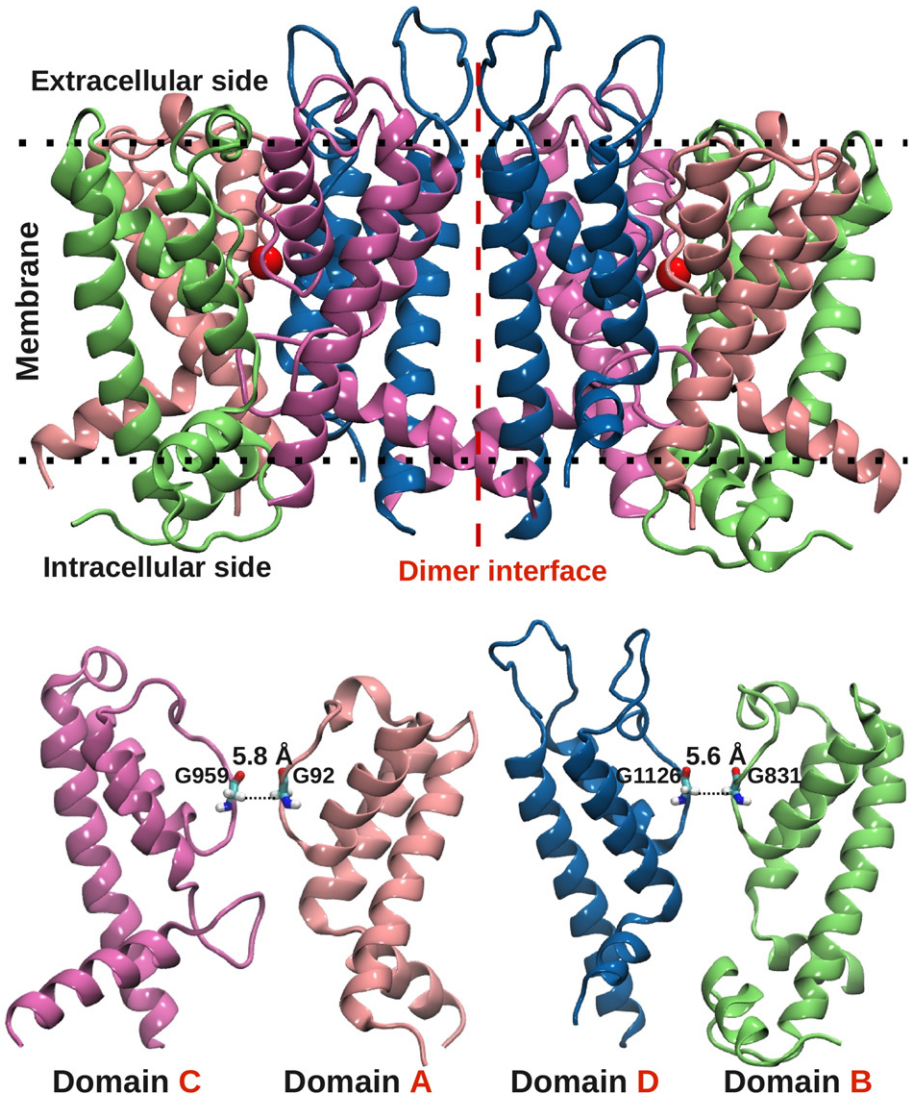

Fig. 3. *Side view representation of the Trk1 model.* The upper panel shows a side view of the modeled dimeric structure of Trk1. The dashed lines indicate the approximate location of lipid head groups. The four repeats of each Trk1 monomer are colored identically: domain A — pale red, domain B — green, domain C — magenta, domain D — blue. The potassium ions in the selectivity filters are shown as red spheres. The lower panel shows side views of the facing domains. The glycine residues of the selectivity filter are shown in stick representation. The average distance between the Cα atoms of the selectivity filter glycines (narrowest part of the pore) is indicated.

KtrB templates suggest the existence of a saltbridge between these residues. The herein reported model predicts such an interaction also for Trk1. The stability and role of the putative salt bridge was analyzed *in silico* using molecular dynamics simulations. The presumed saltbridge between the side chains of K1147 and D79 was found to be stable with a distance of ~3 Å persisting during the whole molecular dynamics trajectory, supporting the hypothesis that it is formed in Trk1 similarly as in TrkH and KtrB (Fig. 10).

To analyze this experimentally, a set of mutants was generated that either neutralized the charges (mutants D79A and K1147A), inverted one of the charges (mutants D79K and K1147D) or swapped the charges via a double mutation (mutant D79K, K1147D). It was expected that similar effects for mutations of both residues on folding and function of the protein were observed. The results of the functional (growth) tests and localization of corresponding Trk1/GFP fusion proteins are shown in Fig. 9. Whereas all mutations including D79 (D79A, D79K, D79K/K1147D) lead to severe folding/targeting defects and consequently to no growth at low [K^+], mutations of K1147 were tolerated better. Although some folding/targeting defects were also observed with K1147A and K1147D, there was some membrane staining seen. Additionally growth tests revealed the presence of functional proteins.

These experimental results are not incompatible with the presumed electrostatic interaction but neither prove the existence nor the non-existence of the saltbridge D79/K1147 in Trk1. However, they highlight the importance of these residues for folding/targeting (and probably structural integrity) of the protein. The significantly stronger effect of mutations at position 79 suggested that D79 might either be structurally more important or additionally interacting with another residue close by. In our initial model the closest residue would be arginine at position 1140 that has a 7 Å distance of its guanidino group to carboxyl-oxygen of D79 and thus might be involved in such an interaction. However, a strain expressing R1140A exhibited no defects in growth, nor was membrane targeting of the corresponding GFP fusion protein affected (not shown). Subsequent molecular dynamics simulations instead revealed a hydrogen-bonding interaction of D79 with R76 located at the loop preceding the P_A helix (Fig. 10). This interaction did not perturb the salt bridge D79-K1147 and was not persistent throughout the trajectory but nevertheless was sampled regularly, even in the later part of the simulation. It thus represents an additional contact. The possible existence of repeatedly occurring bifurcated hydrogen-bonding of D79 to K1147 and R76 could explain the stronger effect of D79 mutations in comparison to K1147 mutations.

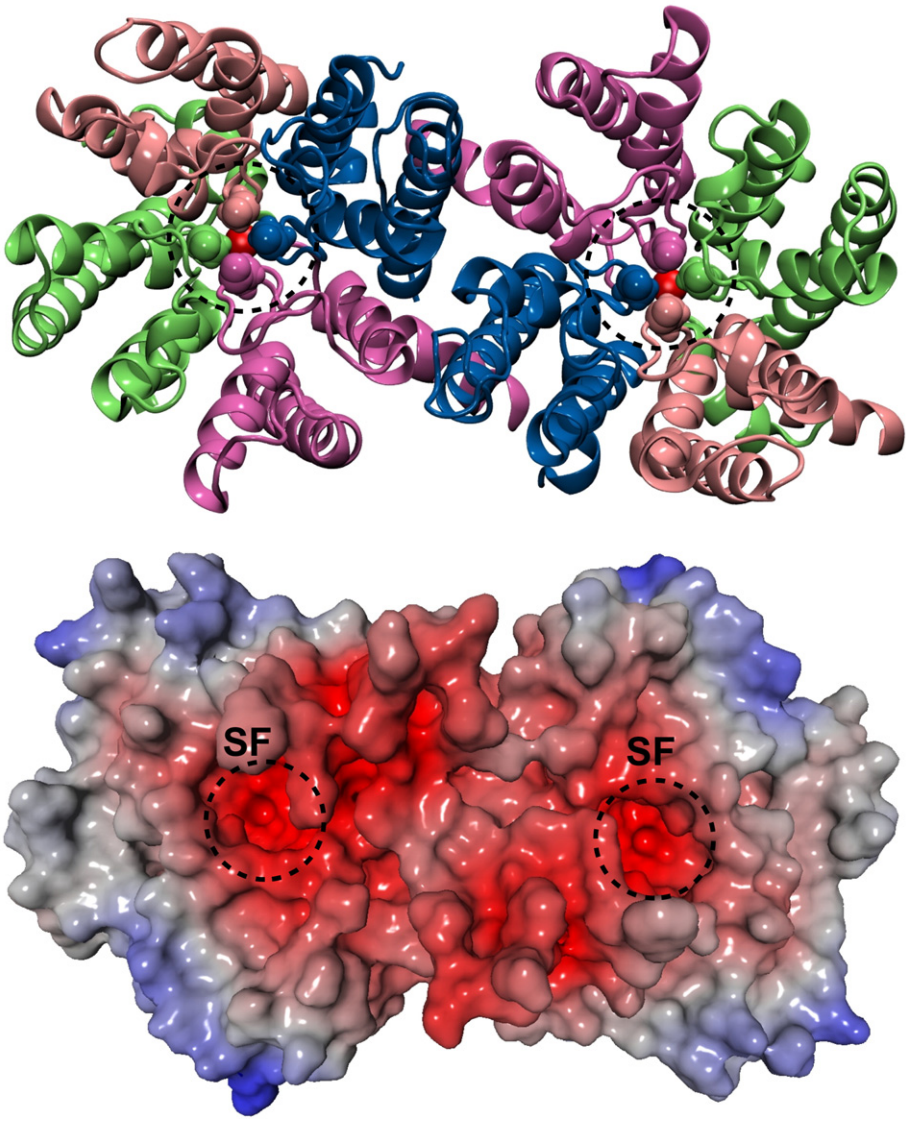

Fig. 4. *Top view of the Trk1 dimer model.* The upper panel shows the top view onto the Trk1 dimer model. The four repeats arranged around the central pore are colored in the same way as in Fig. 3 (domain A — pale red domain B — green, domain C — magenta, domain D — blue). The potassium ions in the selectivity filter are shown as red VdW sphere representation. The glycine residues of the selectivity filter are shown as VdW sphere representation colored according to the corresponding domains. The lower panel shows the top view of the model, colored by electrostatic potential. The location of selectivity filter (SF) is shown by dashed lines. The electrostatic potential is shown from red (negative) to blue (positive) colors.

MD simulations with the (non-functional) double mutant D79K/K1147D and the single mutant K1147A were performed to obtain a better understanding of the effects of these mutations in the described interactions. The results revealed that in the D79K/K1147D double mutant the initially present salt bridge between K79 and D1147 was lost already during equilibration and was never sampled again during the simulation (not shown). In the single mutant, in which the positive charge of K1147 was neutralized (K1147A), the interaction between D79 and R76 transiently observed in the wild type simulations became persistent throughout the whole trajectory (Fig. 10).

Within the $M2_D$ helix a positively charged residue is highly conserved, (lysine 1158 in Trk1, in all other transporters from the family arginine is present at this position). This residue has been proposed to interact with a conserved glutamate (E1117 in Trk1) of the P_D helix. Our model excludes this possibility as both residues are over 15 Å (Cα–Cα distance) apart. The presence of the K1158-E1117 interaction would clearly falsify our model and therefore be a good candidate to scrutinize our prediction. Furthermore, an electrostatic interaction between a lysine at position 1100 (within the loop between $M1_D$ and P_D) with either E1097 or E1117 seemed possible. Additionally, residues E1117 and E1097 ($M1_D$) are within a Cα–Cα distance of 12 Å. An interaction between these two residues would be plausible if one would be oppositely charged. To test for these potential interactions in Trk1, the following set of mutants was constructed: K1158A, K1158R, E1117A, E1097K and E1097A.

Replacement of the conserved positively charged K1158 in $M2_D$ with alanine did not alter function (as assessed by growth tests) nor was any effect on targeting of the GFP fusion protein observed. Consequently, also the K1158R strains did not show difference to Trk1 wt. Our results also argued against an involvement of K1100 in any important structural interaction. Neither function nor targeting of this mutant was affected (not shown). Consistently, the interaction between K1100 with either E1097 or E1117 was never observed in our trajectories.

Glutamate 1117 located next to the selectivity filter contributes to the negative potential above the selectivity filter entry site. Neutralization of this glutamate to alanine led to a growth defect at low [K^+]. Folding and targeting of the corresponding GFP fusion protein seemed only slightly affected. Neutralization of glutamate 1097 (E1097A) that in our model contacts threonine 1143, or charge swapping at this position (E1097K) exerted an even stronger growth defect than the mutation

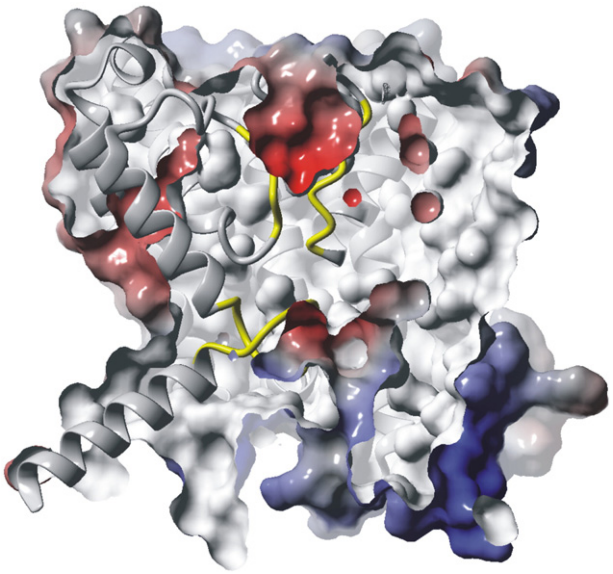

Fig. 5. *Cut through one monomer of Trk1 model*, side view. The two selectivity filter loops and internal loop are shown in yellow color. The electrostatic potential is mapped to the Trk1 surface, color coded from red (negative) to blue (positive).

of E1117 to alanine. Folding/targeting was more severely impaired in E1097K as compared to E1097A (Fig. 11).

We modeled helix $M2_D$ as consisting of two helices connected by a proline containing loop. This helix is straight in K-channels. We wanted to exclude the possibility that this helix would also be a single straight helix in Trk1, therefore differing from the template structure [15]. The proline residues would -in case of a continued helix- represent a deviation from an optimal α-helix and could allow for function associated bending motions. The bending hypothesis implies, that a mutation of this proline would prevent the bending and alter either folding or protein function. Furthermore, if the 90 degree bend is correct one could imagine a change in the bending angle which could be important for "gating" of Trk1. In order to address this question, we mutated a glycine residue (G1161) that is located just two positions before the proline residue in the sequence to a proline (G1161P) to further limit the conformational space potentially sampled by the loop. Insertion of this proline (G1161P) would be compatible with our model and the observed bending angle of 90 degrees, but would further limit additional movements (Fig. 3). Functional testing showed that Trk1[G1161P] grew as well as wt. Fluorescence microscopy analysis did not reveal any obvious defects in folding/targeting of Trk1[G1161]/GFP (Supplementary Fig. 6), suggesting that changes in bending of $M2_D$ are not relevant for gating.

4. Discussion

Fungal Trk proteins belong to a group of cation translocation systems named superfamily of K^+ transporters (SKT proteins) consisting of prokaryotic TRK and Ktr, and eukaryotic HKT and Trk systems [10,8,43,44]. SKT proteins have probably evolved from ancestral K-channels (similar to KcsA from *Streptomyces lividans*) through gene duplication and alterations in gating and/or translocation mechanisms [8]. Functional systems either consist of a membrane protein core with a fourfold repeat of the K-channel "transmembrane helix 1 - pore loop - transmembrane helix 2" (MPM) motif plus an associated hydrophilic subunit or of one polypeptide chain comprising both, the membrane spanning domain and the intracellular hydrophilic domain. The intracellular domain is typically located between the first and the second MPM motif. Regarding their physiological function, K^+ translocation (uptake), SKT proteins could act as monomers. The first structural models [8,10] however, assumed a tetrameric structure to provide a favorable environment for the charged residues within $M2_D$. This notion was experimentally supported by the discovery that *S. cerevisiae* Trk1 can also mediate Cl^- currents [51,52], which could most easily be explained by assuming the existence of a second "metapore" formed at the central interface of four symmetrically arranged monomers. On the other hand, the known crystal structures [14,15,45] show a dimeric composition. Thus, a dimeric composition for Trk1 in our modeling approach was assumed, being aware that a composition of four monomers might be also possible. The SKT proteins vary significantly in selectivity: (i) SKT proteins (protein complexes) can be highly selective for K^+, like yeast Trk1, (ii) some are rather non-specific and do not discriminate between Na^+ and K^+ like TrkH [45], (iii) while others even show some preference for Na^+ over K^+ (AtHKT1, [46]). The mechanism of transport is still enigmatic. Na^+/K^+ and H^+/K^+ symport have been suggested (for review see e.g. [47]). It has been shown recently that KtrAB and TrkH/TrkA can act as channels [45,15]. The driving force utilized by fungal Trk transport systems has not yet been unambiguously identified. For Trk1, the major K^+-uptake system of the yeast *S. cerevisiae* both, K^+/Na^+ symport and H^+/K^+ symport have been discussed [47]. However, the experimental evidence for either mechanism is not fully compelling. Due to the lack of a method to determine the membrane potential of yeast cells with sufficient precision, it has not yet been possible to determine the electrochemical K^+-gradient. Thus, the question whether Trk1 simply acts as facilitator of diffusion (channel) or if it is a secondary or even primary active transporter cannot yet be answered unambiguously. New testable hypotheses can now be

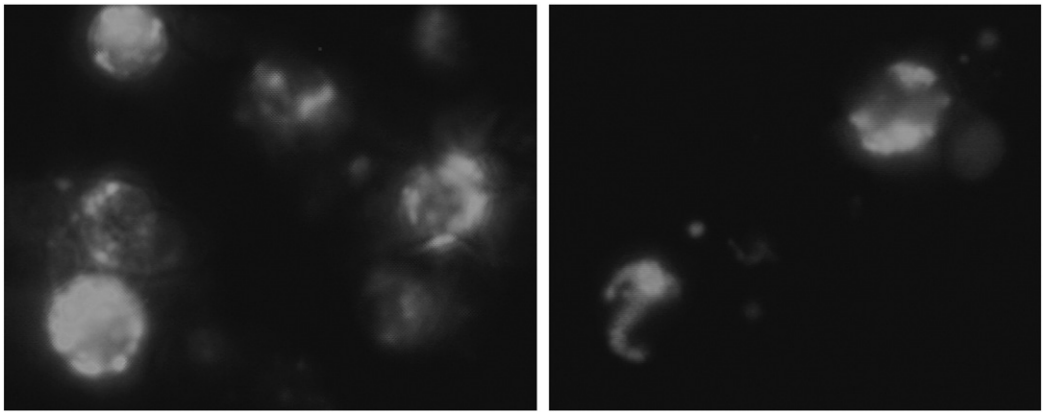

Fig. 6. *Mutation of selectivity filter glycines to leucines impairs folding/membrane targeting of Trk1/GFP fusion proteins.* Left side: Trk1[G959L]/GFP (SF_C), right side: Trk1[G1126L]/GFP (SF_D). Fluorescence microscopy with cells expressing TRK1[G92L]/GFP (SF_A) or TRK1[G831L]/GFP (SF_B) revealed similar patterns of fusion protein distribution, i.e. no proper targeting to the plasma membrane.

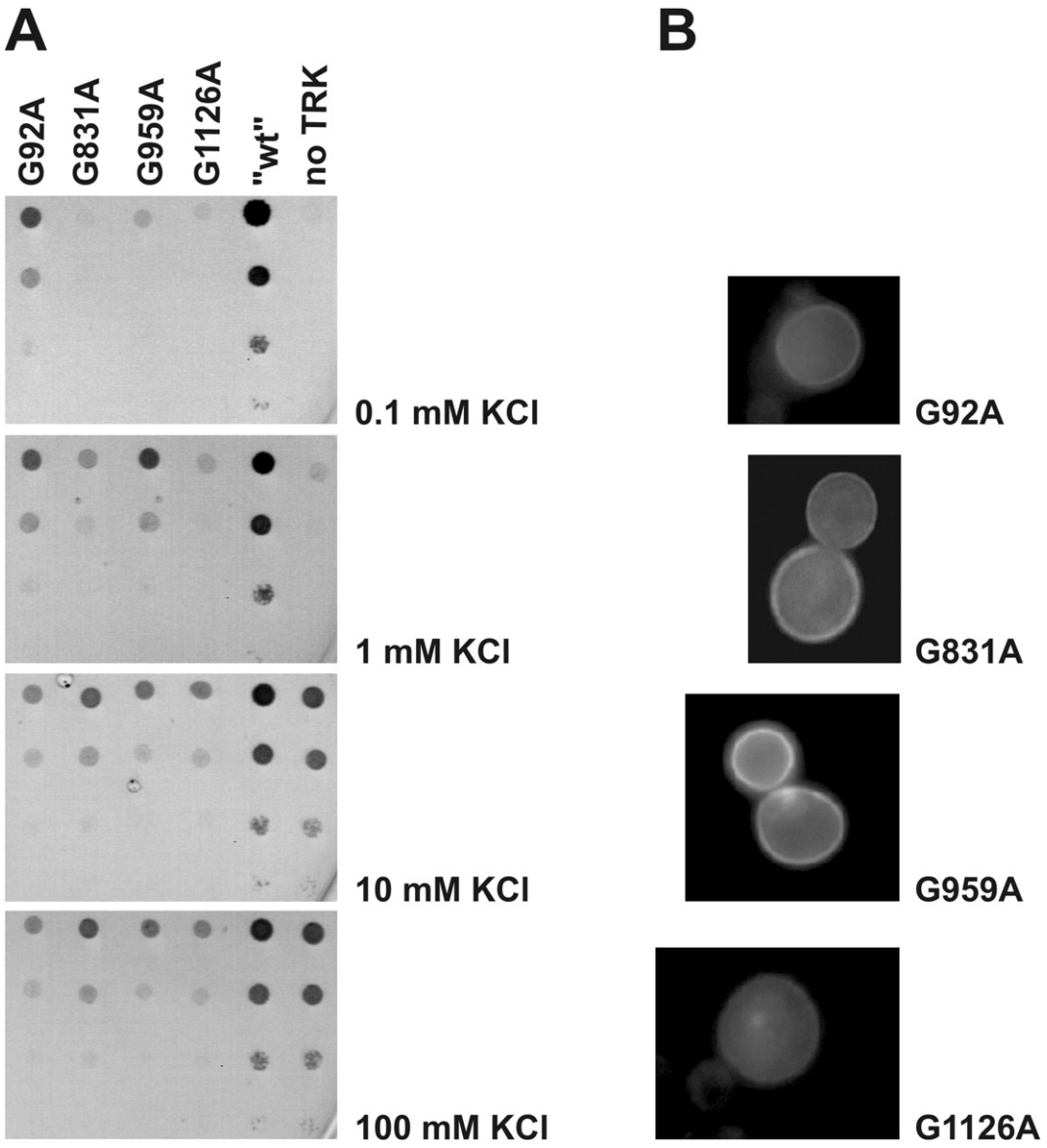

Fig. 7. *A*: *The mutation of each of the selectivity filter glycines to alanine inhibits growth.* Surprisingly, growth defects were not only observed at low [K^+] but also at 100 mM KCl, a concentration at which the functional negative control (no TRK) grows as good as wt. *B*: These mutations do not affect folding/targeting as strong as the corresponding glycine to leucine mutations. Whereas impaired folding and or targeting was sometimes observed with Trk1[G1126A]/GFP, the mutated proteins Trk1[G92A]/GFP, Trk1[G959A]/GFP and Trk1[G831A]/GFP seemed to be mostly folded and targeted correctly.

elaborated based on the structural, functional and dynamics data of this study and recent data from the literature [14,15,45].

Apart from the models developed by Durell and Guy on the basis of the KcSA channel [10], no atomistic structural information of Trk proteins from fungi is available yet. Recently, the structures of two related K^+ translocation systems, TrkH/TrkA from (*Vibrio parahaemolyticus*) [14,45] and KtrAB (from *Bacillus subtilis*, [15]), were reported. Using these structures as templates, we intended to develop a refined atomic scale homology model for the core (i.e. the 4xMPM transmembrane part) structure of Trk1. However, TrkH and KtrB (the proteins corresponding to the Trk1 core) are only loosely related to Trk1 with sequence identities of 11 % and 22 %, respectively. Even though the sequence identity of 22 % allows reasonable homology modeling of membrane proteins [53] any model created using templates with such low sequence identity will remain of medium resolution. To increase the reliability of our models we thus challenged our model by experimental scrutiny in several regions. Glycine to leucine mutations of each of the four glycine residues that form the narrowest part of the selectivity filter in Trk1 strongly affected growth. The reduced growing might result from defects in protein folding or protein targeting. The similarity of the results for each mutant indicates that their position in the four repeats should be similar. The effect of mutation of each of the four glycines indicates that they are located at a functionally and/or structurally critical place. We observed that only the conservative mutation to alanine was tolerated to some extent. The effect was not fully symmetric, as targeting was still strongly affected in the G1126A mutant. Functional analysis by growth tests at low [K^+] revealed that all glycine to alanine mutations affected K^+ uptake (growth) to a different extent. Surprisingly however, also growth at non limiting [K^+], i.e., when "functional negative control" strain cells (that did not express TRK1) grew indistinguishable from TRK1-wt expressing cells, was impaired. This result prompted us to analyze one mutant, G959A (SF_C), in more detail. We observed that cells expressing the G959A mutant were inhibited much stronger by other competing monovalent (NaCl and choline chloride) and divalent cations (Ca^{2+}) as compared to wt cells (Fig. 8). MD simulations revealed that the pore diameter (the glycine-glycine (or glycine-alanine) distance between opposite domains (repeats)) increased from ~5.8 Å to 7.5 Å in G959A. Additionally,

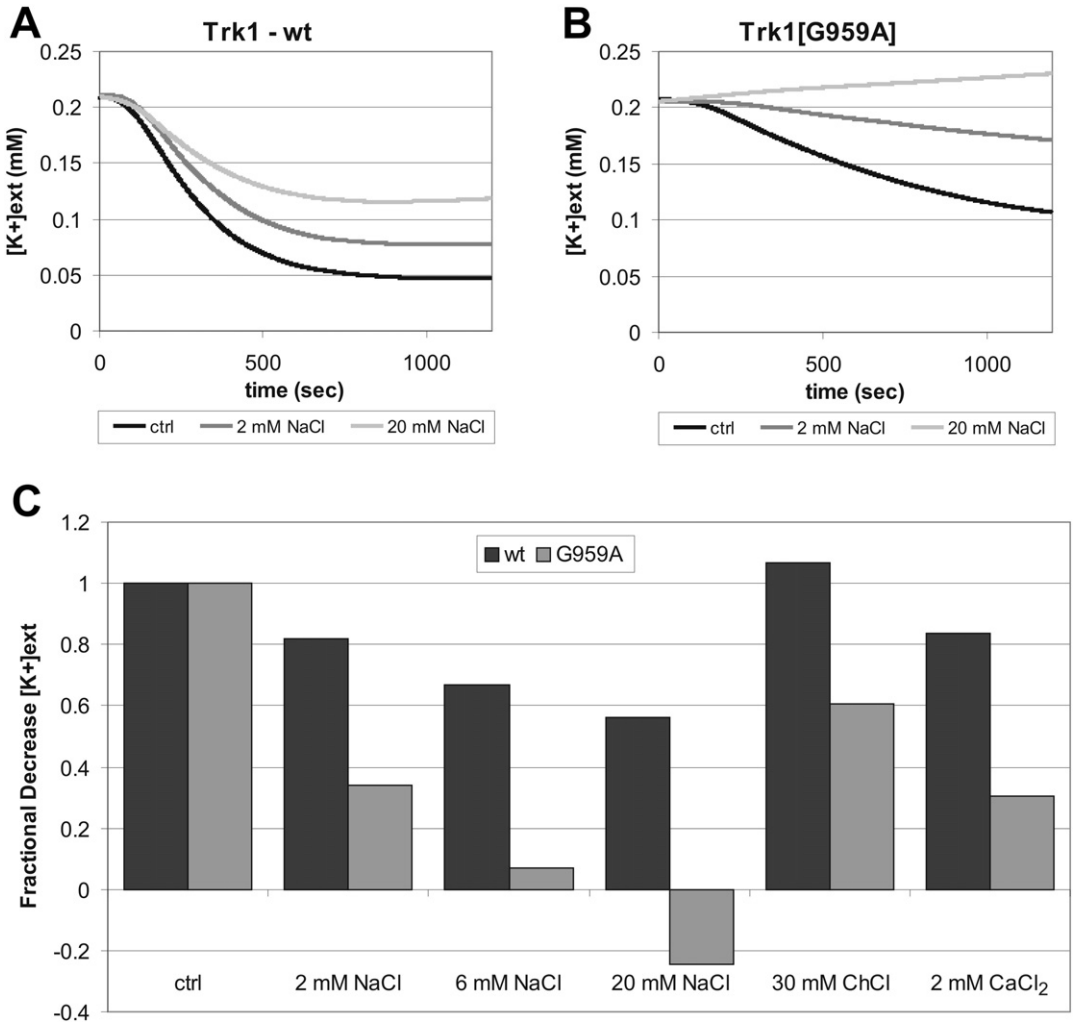

Fig. 8. *K^+-translocation through Trk1-SF_C glycine to alanine mutant (G959A) is strongly inhibited by interfering cations.* A: K^+ decrease in the test solution (pH 5, 0.2 mM KCl) mediated by Trk1 under control conditions (black lines) and with either 2 mM NaCl (gray lines) or 20 mM NaCl added (light gray lines). B: The same experiment carried out with cells expressing TRK1 [G959A]. C: Bar graph showing the relative decrease in [K^+] in 20 min (scaled to the decrease under control conditions) for wt (black bars) and G959A (gray bars) without (ctrl) and different additional cations. K^+ uptake through Trk1-wt was to some degree inhibited by interfering ions (except choline chloride), but the system mediated K^+ uptake under all tested conditions. The inhibition of K^+ uptake Trk1[G959A] by interfering cations is much more pronounced as compared to wt. At 20 mM NaCl, even K^+ efflux was observed. Under none of the tested conditions uptake or efflux was observed with the functional negative control cells (BY4741-3M-fnc; not shown).

higher fluctuations in the 100 ns MD simulations of glycine-glycine (-alanine) distances indicated that the selectivity filter became more flexible. These results are compatible with a reduced selectivity as has been shown for the analogous mutations in the related transporter KtrB [40,41]. Thus, we conclude that these glycine residues are indeed most likely located in the narrowest place of the selectivity filter and that they are important for the structural integrity of the selectivity filter. It is interesting to note that according to the sequence alignment, this position of SF_A domain could tolerate another residue, e.g. serine as found in some HKT proteins. In contrast, the analogous positions in SF_B, SF_C and SF_D are always occupied by glycine. At the level of domains however, differences between sequence patterns of B, C and D domains were observed. While the B and D domains (repeats) possess very regular and conserved residue patterns of pore helices and the selectivity filter, the C domain is not as well conserved among transporter families (TrkH, Trk1,2, HKT). This could suggest difference in evolutionary pressure and is supported by our results which show that the detailed roles of these four residues are not fully identical: Although all glycine mutations had similar effects, we also observed differences. Viz., a considerable amount of G92A (SFA) and G959A (SFC) cells grew at 0.1 or 0.3 mM KCl, whereas the two other SF glycine to alanine mutations almost completely prohibited growth at the same conditions.

Several conserved residues were predicted earlier to form two saltbridges in SKT proteins [8,10,13]. In yeast Trk1, residue E1117 and K1158 would be candidates for forming one of these salt bridges. However, our model predicts that these residues are not close enough to interact, while the distance between E1097 and E1117 would favor an interaction. Growth and localization of mutants E1097K, E1097A, E1117A and K1158A were consistent with our model (Fig. 11). They were inconsistent with an interaction between E1117 and K1158. For the other proposed salt bridge that would be between D79 and K1147 in Trk1, a similar effect of charge neutralization of each interacting residue (D79A or K1147A) would be expected, if they interact solely with each other. However, our experimental results show that all mutations in position 79 completely prohibited correct folding and targeting. Mutations at position 1147 affected folding/targeting but still allowed for surface expression of some functional protein (Fig. 9). The drastic effect of D79 mutations might be caused by the presence of an additional partner (R76), as suggested by the molecular dynamics simulations (Fig. 10).

A not expected property of some mutants, which were designed to only alter function, was the observation of defects in folding/targeting. This demonstrates the general sensitivity of the folding process of Trk1 to perturbations in critical regions. A possible explanation could

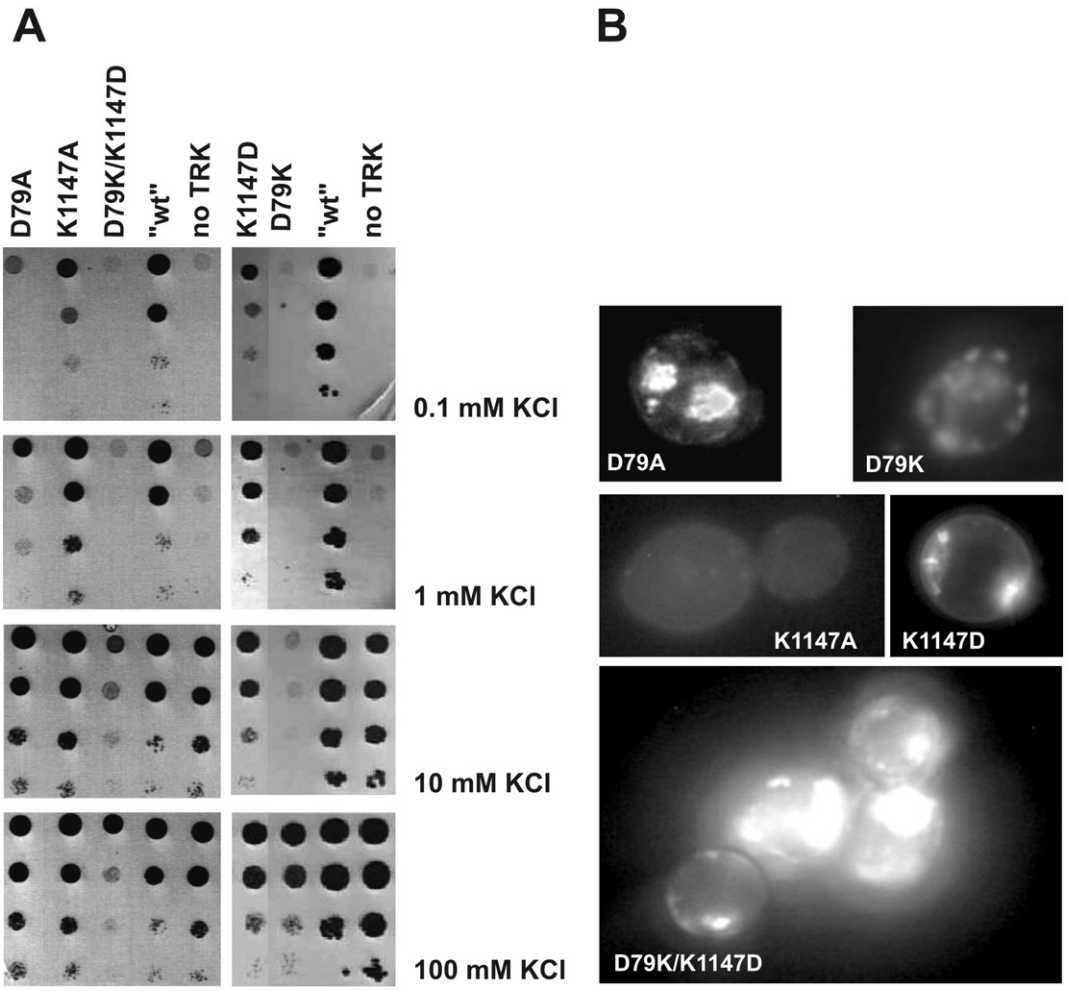

Fig. 9. *A: Neutralization or charge swapping of the salt bridge forming D79 and K1147 in TrkH, TrkB and in our Trk1 model leads to growth defects at low* [K^+]. When lysine 1147 was mutated to alanine or aspartic acid (K1147A, K1147D), some growth at low [K^+] was observed. However, single mutations of D79 (D79A, D79K) or charge swapping (D79K/K1147D) completely abolished growth at low [K^+]. and even to some degree under "permissive" [KCl] (10 mM and 100 mM) at which specific K^+-uptake is not necessary for growth. B: The mutations also lead to improper targeting. However when lysine 1147 was mutated to either alanine or aspartic acid, some membrane staining was observed for the corresponding Trk1/GFP fusion proteins. This is consistent with the growth test results (A) that also showed the presence of some functional protein.

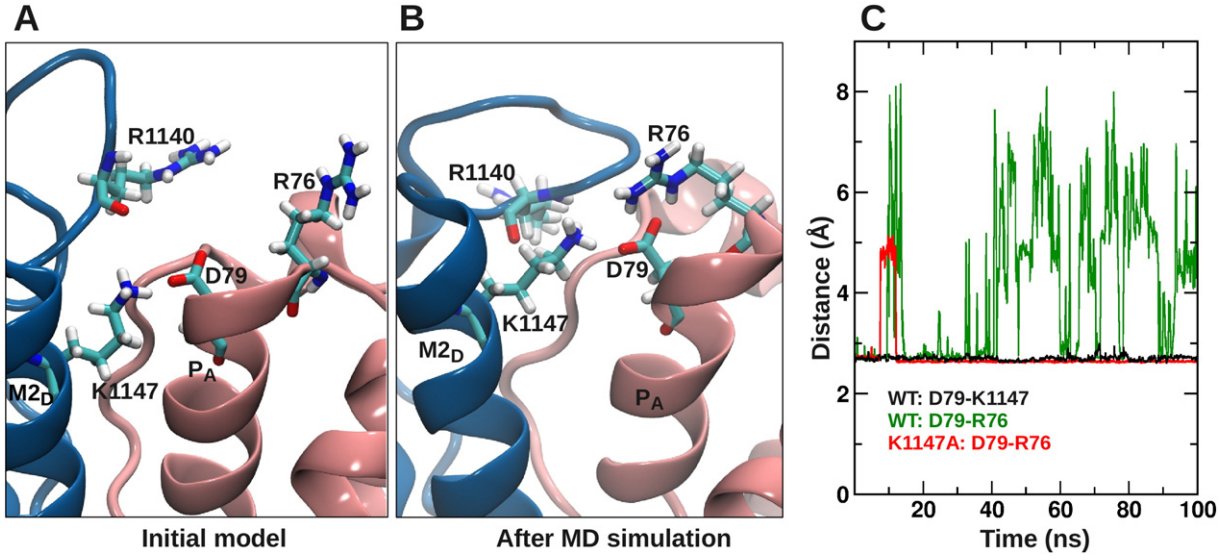

Fig. 10. *Detailed view of mutated residues.* A and B show the positions of residues K1147 ($M2_D$) and D79 (P_A) putatively involved in forming a salt bridge before (A) and after MD simulation (B). Note that in the initial model a contact of D79 and R1140 seemed possible, whereas during MD simulation repeatedly transient contacts between D79 and R76 seemed to be established. C: Closest nitrogen-oxygen distances between wt D79 and K1147 (black), wt D79 and R76 (green) and between D79 and R76 in the K1147A mutant (red). Distances were measured every 2 ps and plotted as the sliding average over 200 ps.

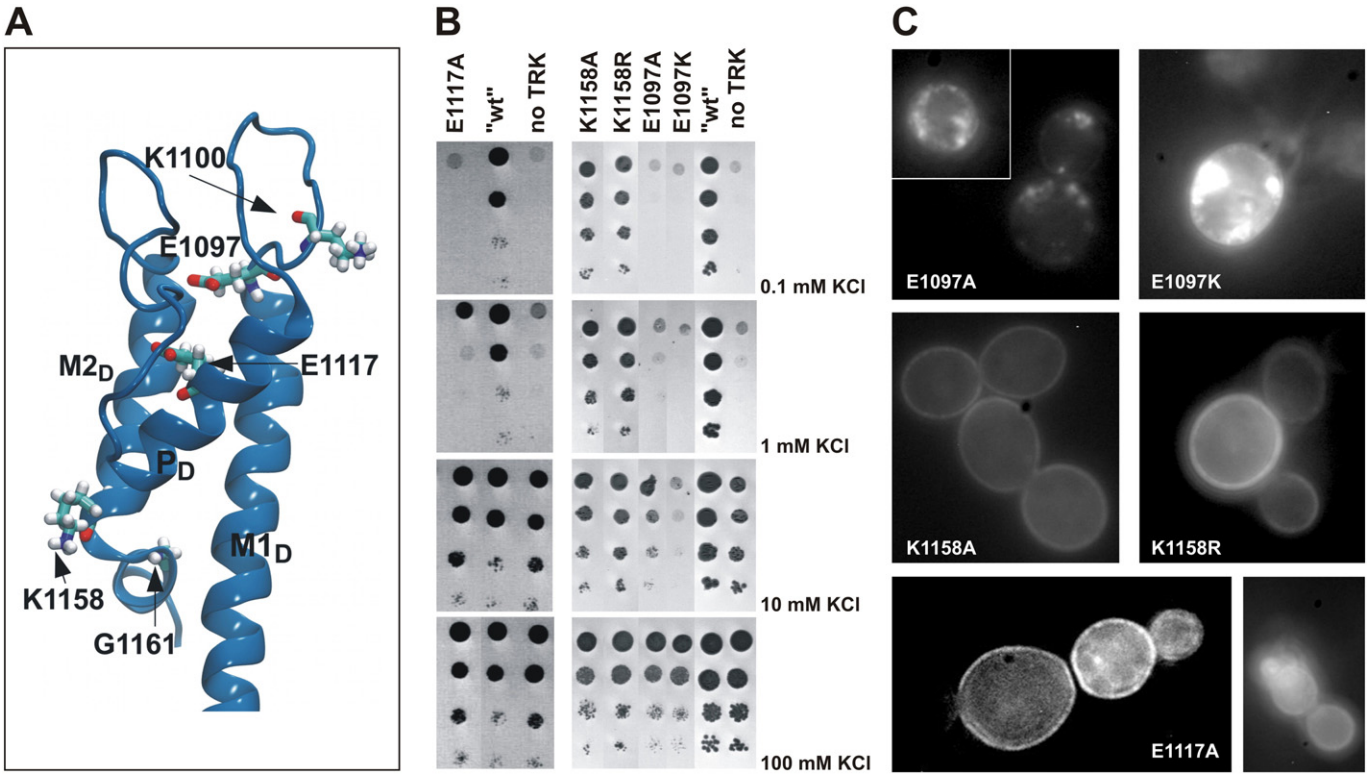

Fig. 11. *Effects of mutations of charged residues in domain D.* A: Localization (stick representation) of residues (at the end of molecular dynamics simulation trajectory) within domain D that were mutated during the study. For details see text. B: Functional (growth) tests. Neutralization of E1117 in MP_D (E1117A) or E1097 at the end of $M1_D$ (E1097A) as well as opposing the charge of E1097 (E1097K) led to growth defects on low [K^+] plates. C: Localization of the corresponding Trk1/GFP fusion proteins. Targeting of E1097A/GFP and E1097A/GFP (to a lower degree) was compromised. The mutation of K1158 to arginine as present in all other members of the SKT family, or neutralizing (K1158A) did not influence growth (B) nor was its folding/targeting affected (C).

be the difficulty to fold the four repeats on one amino acid chain, compared to the assembly of four monomers as in K-channels. However, that mutants in uncritical regions do not influence the folding. For example, mutation of arginine 1140 (located in a loop and exposed to the solvent in our model) to alanine (R1140A) as well as K1158R and K1158A did neither show growth nor folding/targeting defects.

Finally, it can be concluded that the discussed structural model correctly represents key features of Trk1 and is consistent with the experimental data so far. As protein folding seems to be a critical issue for Trk1 and mutations easily lead to folding defects, the model might serve in the future to predict modest mutations that nevertheless would lead to measurable alterations of Trk1 function. Our model provides first experimentally validated structural evidence of the Trk1 structure. A charged ion permeation path with a selectivity filter similar to that of ion channels is observed in the model. The permeation path becomes then obstructed or regulated by a proline containing loop structure in the center of the membrane spanning region. The herein reported Trk1 model can serve as an important platform for hypothesis generation to further investigate K^+ uptake to unambiguously answer the question of active vs. passive transport.

Supplementary data to this article can be found online at http://dx.doi.org/10.1016/j.bbamem.2015.02.007.

Acknowledgements

This work was supported by German BMBF grant FKZ 0315786B (Translucent2) within the SysMO2 ERANET (JL). VZ, SP and RE were supported by the Czech Science Foundation grant 13-21053S. The authors wish to thank Blanca Randel for excellent technical assistance and Maik Kschischo and Matthias Kahm for providing the R-script to smooth raw K^+-flux data. The help of Saskia Holweg, Alexandra Hübner, Katja Kehl, Christina Julius and Daniel Ganser with some experiments is highly appreciated.

References

[1] L.Y. Jan, Y.N. Jan, Voltage-gated potassium channels and the diversity of electrical signalling, J. Physiol. 590 (2012) 2591–2599.
[2] J. Ariño, J. Ramos, H. Sychrová, Alkali metal cation transport and homeostasis in yeasts, Microbiol. Mol. Biol. Rev. 74 (2010) 95–120.
[3] M.B. Wright, J. Ramos, M.J. Gomez, K. Moulder, M. Scherrer, G. Munson, R.F. Gaber, Potassium transport by amino acid permeases in *Saccharomyces cerevisiae*, J. Biol. Chem. 272 (1997) 13647–13652.
[4] R. Madrid, M.J. Gómez, J. Ramos, A. Rodríguez-Navarro, Ectopic potassium uptake in trk1 trk2 mutants of *Saccharomyces cerevisiae* correlates with a highly hyperpolarized membrane potential, J. Biol. Chem. 273 (1998) 14838–14844.
[5] H. Bihler, C.L. Slayman, A. Bertl, Low-affinity potassium uptake by *Saccharomyces cerevisiae* is mediated by NSC1, a calcium-blocked non-specific cation channel, Biochim. Biophys. Acta 1558 (2002) 109–118.
[6] R.F. Gaber, C.A. Styles, G.R. Fink, TRK1 encodes a plasma membrane protein required for high-affinity potassium transport in *Saccharomyces cerevisiae*, Mol. Cell. Biol. 8 (1988) 2848–2859.
[7] A. Bertl, J. Ramos, J. Ludwig, H. Lichtenberg-Frate, J. Reid, H. Bihler, F. Calero, P. Martinez, P.O. Ljungdahl, Characterization of potassium transport in wild-type and isogenic yeast strains carrying all combinations of *trk1*, *trk2* and *tok1* null mutations, Mol. Microbiol. 47 (2003) 767–780.
[8] S.R. Durell, Y. Hao, T. Nakamura, E.P. Bakker, H.R. Guy, Evolutionary relationship between K^+ channels and symporters, Biophys. J. 77 (1999) 775–788.
[9] D.A. Doyle, J.M. Cabral, R.A. Pfuetzner, A. Kuo, J.M. Gulbis, S.L. Cohen, B.T. Chait, R. MacKinnon, The structure of the potassium channel: molecular basis of K^+ conduction and selectivity, Science 280 (1998) 69–77.
[10] S.R. Durell, H.R. Guy, Structural models of the KtrB, TrkH, and Trk1,2 symporters based on the structure of the KcsA K^+ channel, Biophys. J. 77 (1999) 789–807.
[11] R. Haro, A. Rodríguez-Navarro, Molecular analysis of the mechanism of potassium uptake through the TRK1 transporter of *Saccharomyces cerevisiae*, Biochim. Biophys. Acta 1564 (2002) 114–122.

[12] R. Haro, A. Rodríguez-Navarro, Functional analysis of the M2D helix of the TRK1 potassium transporter of *Saccharomyces cerevisiae*, Biochim. Biophys. Acta Biomembr. 1613 (2003) 1–6.
[13] N. Kato, M. Akai, L. Zulkifli, N. Matsuda, Y. Kato, S. Goshima, A. Hazama, M. Yamagami, H.R. Guy, N. Uozumi, Role of positively charged amino acids in the M2 D transmembrane helix of Ktr/Trk/HKT type cation transporters, Channels 1 (2007) 161–171.
[14] Y. Cao, X. Jin, H. Huang, M.G. Derebe, E.J. Levin, V. Kabaleeswaran, Y. Pan, M. Punta, J. Love, J. Weng, M. Quick, S. Ye, B. Kloss, R. Bruni, E. Martinez-Hackert, W.A. Hendrickson, B. Rost, J.A. Javitch, K.R. Rajashankar, Y. Jiang, M. Zhou, Crystal structure of a potassium ion transporter TrkH, Nature 471 (2011) 336–340.
[15] R.S. Vieira-Pires, A. Szollosi, J.H. Morais-Cabral, The structure of the KtrAB potassium transporter, Nature 496 (2013) 323–328.
[16] A. Rodríguez-Navarro, J. Ramos, Dual system for potassium transport in *Saccharomyces cerevisiae*, J. Bacteriol. 159 (1984) 940–945.
[17] K.F. Doheny, P.K. Sorger, A.A. Hyman, S. Tugendreich, F. Spencer, P. Hieter, Identification of essential components of the *S. cerevisiae* kinetochore, Cell 73 (1993) 761–774.
[18] S.N. Ho, H.D. Hunt, R.M. Horton, J.K. Pullen, L.R. Pease, Site-directed mutagenesis by overlap extension using the polymerase chain reaction, Gene 77 (1989) 51–59.
[19] R.D. Gietz, R.H. Schiestl, High-efficiency yeast transformation using the LiAc/SS carrier DNA/PEG method, Nat. Protoc. 2 (2007) 31–34.
[20] M.A. Larkin, G. Blackshields, N.P. Brown, R. Chenna, P.A. McGettigan, H. McWilliam, F. Valentin, I.M. Wallace, A. Wilm, R. Lopez, J.D. Thompson, T.J. Gibson, D.G. Higgins, Clustal W and Clustal X version 2.0, Bioinformatics 23 (2007) 2947–2948.
[21] C. Notredame, D.G. Higgins, J. Heringa, T-Coffee: a novel method for fast and accurate multiple sequence alignment, J. Mol. Biol. 302 (2000) 205–217.
[22] F. Armougom, S. Moretti, O. Poirot, S. Audic, P. Dumas, B. Schaeli, V. Keduas, C. Notredameet, Expresso: automatic incorporation of structural information in multiple sequence alignments using 3D-Coffee, Nucleic Acids Res. 34 (2006) 604–608.
[23] A. Sali, T.L. Blundell, Comparative protein modelling by satisfaction of spatial restraints, J. Mol. Biol. 234 (1993) 779–815.
[24] R.A. Laskowski, M.W. MacArthur, D.S. Moss, J.M. Thornton, PROCHECK: a program to check the stereochemical quality of protein structures, J. Appl. Crystallogr. 26 (1993) 283–291.
[25] M. Shen, M. Sali, Statistical potential for assessment and prediction of protein structures, Protein Sci. 15 (2006) 2507–2524.
[26] M. Wiederstein, M.J. Sippl, ProSA-web: interactive web service for the recognition of errors in three-dimensional structures of proteins, Nucleic Acids Res. 35 (2007) 407–410.
[27] C. Kandt, W.L. Ash, D.P. Tieleman, Setting up and running molecular dynamics simulations of membrane proteins, Methods 41 (2007) 475–488.
[28] O. Berger, O. Edholm, F. Jähnig, Molecular dynamics simulations of a fluid bilayer of dipalmitoylphosphatidylcholine at full hydration, constant pressure, and constant temperature, Biophys. J. 72 (1997) 2002–2013.
[29] W.L. Jorgensen, D. Maxwell, J. Tirado-Rives, Development and testing of the OPLS all-atom force field on conformational energetics and properties of organic liquids, J. Am. Chem. Soc. 118 (1996) 11225–11236.
[30] C. Neale, R. Pomès, Combination rules for united-atom lipids and OPLSAA proteins, http://www.pomeslab.com/files/lipidCombinationRules.pdf2006.
[31] H.J.C. Berendsen, J.P.M. Postma, W.F. van Gunsteren, J. Hermans, Interaction models for water in relation to protein hydration, in: B. Pullman (Ed.), Intermolecular Force, D. Reidel Publishing Company, 1981, pp. 331–342.
[32] D. Van Der Spoel, E. Lindahl, B. Hess, G. Groenhof, A.E. Mark, H.J. Berendsen, GROMACS: fast, flexible, and free, J. Comput. Chem. 26 (2005) 1701–1718.
[33] B. Hess, C. Kutzner, D. van der Spoel, E. Lindahl, GROMACS 4: algorithms for highly efficient, load-balanced, and scalable molecular simulation, J. Chem. Theory Comput. 4 (2008) 435–447.
[34] S. Pronk, S. Páll, R. Schulz, P. Larsson, P. Bjelkmar, R. Apostolov, M.R. Shirts, J.C. Smith, P.M. Kasson, D. van der Spoel, B. Hess, E. Lindahl, GROMACS 4.5: a high-throughput and highly parallel open source molecular simulation toolkit, Bioinformatics 29 (2013) 845–854.
[35] H.J.C. Berendsen, J.P.M. Postma, W.F. van Gunsteren, A. DiNola, J.R. Haak, Molecular dynamics with coupling to an external bath, J. Chem. Phys. 81 (1984) 3684–3690.
[36] B. Hess, H. Bekker, H.J.C. Berendsen, J.G.E.M. Fraaije, LINCS: a linear constraint solver for molecular simulations, J. Comput. Chem. 18 (1997) 1463–1472.
[37] T. Darden, D. York, L. Pedersen, Particle mesh Ewald: an N·log(N) method for Ewald sums in large systems, J. Chem. Phys. 98 (1993) 10089–10092.
[38] M. Mülleder, F. Capuano, P. Pir, S. Christen, U. Sauer, S.G. Oliver, M. Ralser, A prototrophic deletion mutant collection for yeast metabolomics and systems biology, Nat. Biotechnol. 30 (2012) 1176–1178.
[39] Reche, The SIAS server, http://imed.med.ucm.es/Tools/sias.html2008.
[40] N. Tholema, E.P. Bakker, A. Suzuki, T. Nakamura, Change to alanine of one out of four selectivity filter glycines in KtrB causes a two orders of magnitude decrease in the affinities for both K^+ and Na^+ of the Na^+ dependent K^+ uptake system KtrAB from *Vibrio alginolyticus*, FEBS Lett. 450 (1999) 217–220.
[41] N. Tholema, M. Vor der Brüggen, P. Mäser, T. Nakamura, J.I. Schroeder, H. Kobayashi, N. Uozumi, E.P. Bakker, All four putative selectivity filter glycine residues in KtrB are essential for high affinity and selective K^+ uptake by the KtrAB system from *Vibrio alginolyticus*, J. Biol. Chem. 280 (2005) 41146–41154.
[42] P. Mäser, Y. Hosoo, S. Goshima, T. Horie, B. Eckelman, K. Yamada, K. Yoshida, E.P. Bakker, A. Shinmyo, S. Oiki, J.I. Schroeder, N. Uozumi, Glycine residues in potassium channel-like selectivity filters determine potassium selectivity in four-loop-per-subunit HKT transporters from plants, Proc. Natl. Acad. Sci. U. S. A. 99 (2002) 6428–6433.
[43] C. Corratgé-Faillie, M. Jabnoune, S. Zimmermann, A.A. Véry, C. Fizames, H. Sentenac, Potassium and sodium transport in non-animal cells: the Trk/Ktr/HKT transporter family, Cell. Mol. Life Sci. 67 (2010) 2511–2532.
[44] E.J. Levin, M. Zhou, Recent progress on the structure and function of the TrkH/KtrB ion channel, Curr. Opin. Struct. Biol. 27 (2014) 95–101.
[45] Y. Cao, Y. Pan, H. Huang, X. Jin, E.J. Levin, B. Kloss, M. Zhou, Gating of the TrkH ion channel by its associated RCK protein TrkA, Nature 496 (2013) 317–322.
[46] N. Uozumi, E.J. Kim, F. Rubio, T. Yamaguchi, S. Muto, A. Tsuboi, E.P. Bakker, T. Nakamura, J.I. Schroeder, The *Arabidopsis* HKT1 gene homolog mediates inward Na^+ currents in *Xenopus laevis* oocytes and Na^+ uptake in *Saccharomyces cerevisiae*, Plant Physiol. 122 (2000) 1249–1260.
[47] A. Rodríguez-Navarro, Potassium transport in fungi and plants, Biochim. Biophys. Acta 1469 (2000) 1–30.
[48] C.B. Brachmann, A. Davies, G.J. Cost, E. Caputo, J. Li, P. Hieter, J.D. Boeke, Designer deletion strains derived from *Saccharomyces cerevisiae* S288C: a useful set of strains and plasmids for PCR-mediated gene disruption and other applications, Yeast 14 (1998) 115–132.
[49] J. Zahrádka, H. Sychrová, Plasma-membrane hyperpolarization diminishes the cation efflux via Nha1 antiporter and Ena ATPase under potassium-limiting conditions, FEMS Yeast Res. 12 (2012) 439–446.
[50] S. Petrezsélyová, J. Ramos, H. Sychrová, Trk2 transporter is a relevant player in K^+ supply and plasma-membrane potential control in *Saccharomyces cerevisiae*, Folia Microbiol. 56 (2011) 23–28.
[51] T. Kuroda, H. Bihler, E. Bashi, C.L. Slayman, A. Rivetta, Chloride channel function in the yeast TRK-potassium transporters, J. Membr. Biol. 198 (2004) 177–192.
[52] A. Rivetta, T. Kuroda, C.L. Slayman, Anion currents in yeast K^+ transporters (TRK) characterize a structural homologue of ligand-gated ion channels, Pflugers Arch. 462 (2011) 315–330.
[53] M. Punta, L.R. Forrest, H. Bigelow, A. Kernytsky, K. Lin, B. Rost, Membrane protein prediction methods, Methods 41 (2007) 460–474.